EL SEVIER

Contents lists available at ScienceDirect

# Ain Shams Engineering Journal

journal homepage: https://www.sciencedirect.com



# Full Length Article

# Peatland forest monitoring and management solution in Peninsular Malaysia: Optimal parameters for LoRa data



Nordin Ramli d, D

- <sup>a</sup> Wireless and Photonics Networks Research Centre (WiPNET), Department of Computer and Communications System Engineering, Faculty of Engineering, Universiti Putra Malaysia, 43400 UPM Serdang, Selangor, Malaysia
- <sup>b</sup> Institute of Mathematical Research (INSPEM), Universiti Putra Malaysia, 43400 UPM Serdang, Selangor, Malaysia
- c Institute of Tropical Forestry and Forest Products (INTROP), Universiti Putra Malaysia, 43400 UPM Serdang, Selangor, Malaysia
- d Wireless Innovation Lab, Corporate Technology, MIMOS Berhad Taman Teknologi Malaysia, 57000 Kuala Lumpur, Malaysia

#### ARTICLE INFO

# Keywords: Peatland restoration and management Fresnel zone LoRa Remote sensor IoT RSSI

#### ABSTRACT

Peatland forest fires threaten biodiversity, ecosystems, and human health in Southeast Asia, especially during the dry season. Limited in-situ data collection necessitates Long Range (LoRa) sensor-based remote monitoring for its long-range communication, low power consumption, and cost-effectiveness. However, dense vegetation affects Low-Power Wide Area Network (LPWAN) signal propagation through scattering, reflection, and diffraction, impacting data transmission. This study investigates LoRa RF propagation in peatland environments through a measurement campaign at Raja Musa Forest Reserve (RMFR), Selangor. File transfer success rate (FT%) across various land-cover types was analyzed using six Data Rate (DR) and Spreading Factor (SF) configurations. Results show that DR5/SF7 and DR0/SF12 achieve over 80% FT% in moderate and dense vegetation, respectively. The findings enhance LoRa RF planning in challenging ecosystems, offering practical guidelines to improve data transmission reliability in RMFR and other peatlands.

# 1. Introduction

Peatland areas play a crucial role in fulfilling a wide range of essential ecological functions, including water storage, carbon sequestration, and biodiversity conservation. Despite covering only approximately 2.84% of the global land area, peatlands store 10% of the world's freshwater and a substantial amount of hydrocarbons [1]. These ecosystems are characterized by a unique dome-shaped terrain, which supports biomass accumulation from centuries of organic decomposition [2]. Tropical peatlands also serve as genetic reservoirs for valuable plant species and vital wildlife habitats. However, increasing deforestation has severely impacted these ecosystems, leading to biodiversity loss and ecosystem degradation [1].

In Southeast Asia (SEA), human activities such as deforestation and land conversion have exacerbated peatland degradation, leaving them prone to fires during dry seasons. These fires, particularly during El Nino events, contribute to significant carbon emissions and environmental damage [3–6]. Local practices, such as open burning for agriculture, further increase fire risks [7]. Additionally, peat subsidence from drainage intensifies these vulnerabilities by lowering the water table, further destabilizing the ecosystem [8]. The resulting fires have wide-ranging impacts, including health issues [9], economic losses [10], and social challenges [11,12].

Peatland monitoring and restoration, *Greta. C. Dargie et al.* [13] identified four distinguishing features: 1) low vegetation species richness, 2) distinctive vegetation structure, 3) distinctive topography, and 4) high water table. Often, lack access to power grids and cellular networks. Traditional in-situ methods for measuring groundwater levels (GWL) are labor-intensive and difficult to scale. Recent advances, such as the integration of Low-Power Wide-Area Networks (LPWAN) with sensors,

E-mail addresses: nurluqman@upm.edu.my (N.L. Saleh), aduwati@upm.edu.my (A. Sali).

https://doi.org/10.1016/j.asej.2025.103374

Received 17 October 2024; Received in revised form 15 February 2025; Accepted 20 March 2025

<sup>\*</sup> Corresponding author.

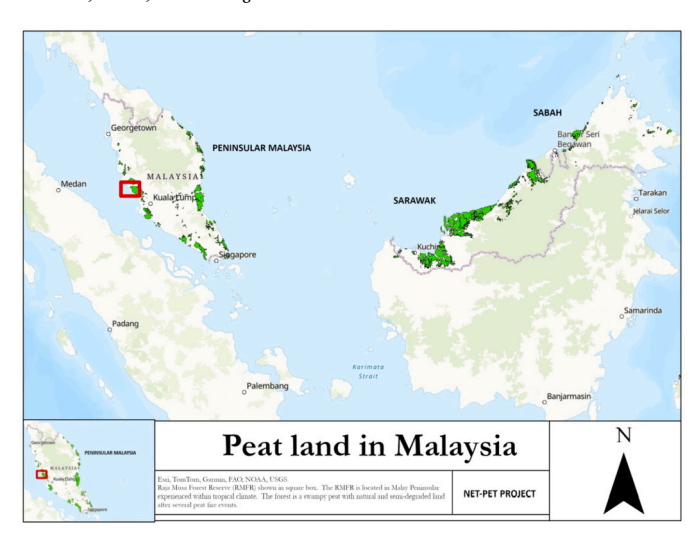


Fig. 1. Location of Raja Musa Forest Reserved (RMFR) in Selangor, Malaysia.

offer promising solutions for remote monitoring [14]. For example, studies have demonstrated the use of LoRa-based sensors to monitor GWL and predict fire danger using advanced models like the Canadian Fire Weather Index [15]. A brief regarding LoRa, which is part of LPWAN technology, will be described in Section 2.1.

At present, monitoring efforts in Malaysia's peatlands remain limited [16,17], particularly due to insufficient expertise in deploying LoRa technology for these specific environments. Existing studies on LoRa have primarily focused on urban and suburban areas [18–21] or specific localized environments like estuaries and forests [22–25]. There remains a critical gap in understanding LoRa's performance in peat swamp forests, particularly in Malaysia.

This study aims to address this gap by evaluating the optimal Data Rate (DR) and Spreading Factor (SF) configurations for reliable LoRa data transmission in the Raja Musa Forest Reserve (RMFR), as shown in Fig. 1. The findings contribute to refining LoRa RF planning strategies for challenging environments, ensuring robust data transmission for environmental monitoring and resource management, not only within RMFR but also in other peatland ecosystems worldwide, supporting large-scale conservation and monitoring efforts beyond the context of Peninsular Malaysia.

# 1.1. Contributions

In line with the Malaysian government's mandate to utilize innovative technologies for forest fire management [26], this study contributes:

- A novel Fresnel Zone model is proposed, incorporating vegetationspecific parameters and propagation characteristics observed in the RMFR ecosystem.
- Evaluation of LoRa performance metrics through a measurement campaign to determine file transfer success rates at different landcovers within RMFR.
- Optimal DR/SF pairing configuration for reliable LoRa data transmission at different land-covers within RMFR.

The rest of the paper is organized as follows: A brief introduction and a literature review are given in Section 1. Section 2.1 reviewed related studies that employ low-power wireless area network (LPWAN) technology including LoRa, specifically Section 2.2 LoRa propagation and Section 2.3 LoRa DR/SF. The characteristics of signal transmission and propagation, including the RSSI, SNR, and Fresnel Zone are explained in Section 3. Section 4 describes the experimental methodology. The experimental results are presented in Section 5. Finally, the findings are discussed in Section 6.

#### 2. Related works

The diversity of peatland forests varies in different climatic zones and holds discrete vegetation formations on different continents [27]. As a result, the strategy for mapping peatland areas varies by continent [28]. Based on references [27,28], it can be concluded that the vegetation formations in peatland forests are unique in different climatic zones and continents. Mainly, vegetation formations at different regions affect the wireless signal propagation and hence the LoRa performance, which is unique to the specific location. This section aims to contribute to the field by reviewing recent propagation studies of in-situ LoRa performance, building upon existing knowledge, and filling a gap in the literature.

#### 2.1. Motivation in peatland forest restoration

In recent years, international bodies have taken a global initiative to restore, monitor, and manage peatland forests under the United Nations (UN) 17 Sustainable Development Goals (SDG). This peatland forest restoration falls under the Climate Action and Life on Land categories under the SDG. Simultaneously, a handbook for peatland mapping and monitoring was published in 2020, providing methodologies and solutions to peatland mapping and monitoring challenges, especially in developing countries [12].

Furthermore, the article reviewed in [29] offers an in-depth analysis of the literature on the management and rehabilitation of peatlands, incorporating diverse strategies and policies. It is worth noting that S. Monteverde et al. work also emphasize the consequences of limited funding, which often results in lagging progress in peatland management. Reed et al. highlighted the substantial financial implications of peatland management and the effects of peatland changes on the allocation of ecosystem services [30]. Their analysis suggests the replication of a similar co-existing method for comparable purposes. In 2019, UN Environment Assembly urged UNEP and Ramsar Convention to establish a global peatland inventory and record interventions, aligning with Ramsar Resolution XIII.13 on remote sensing and geophysical surveys (UNEP, 2019) [31]. By utilizing technological innovations like remote sensing-based systems, local authorities can expand the scope of peatland management and restoration, adopting a broader perspective with specific, measurable, achievable, relevant, and time-bound (SMART) goals [32].

# 2.2. Technical setup in peatland forest restoration

Numerous studies have utilized remote sensing-based systems, including satellites (microwave sensors) and light detection and ranging (LiDAR), for peatland restoration and management tasks. Satellites rely on the backscatter signal and employ synthetic aperture radar (SAR) processing for mapping and imaging, as documented in [33-35]. This method is preferred due to its ability to provide up-to-date information and good resolution across multiple spatial scales for soil mapping. Satellites can also detect hotspots in peatland, providing additional analytic input for managing forest fires [36]. However, microwave sensors, including satellites, are susceptible to scattering and propagating effects. The peatland canopy acts as a large umbrella, attenuating the backscatter signal received by satellites, which degrades the mapping and imaging resolution. Therefore, analyzing the appropriate wavelength is crucial to ensure the signal can penetrate the canopy for effective imaging production [37]. LiDAR is also used for similar purposes, offering highresolution imaging up to one meter in spatial resolution [38]. However, LiDAR has limited mapping capabilities compared to satellites in terms of range sensing. Despite the detailed surface properties provided by these sensors, the in-situ method remains the only way to gather groundwater level (GWL) data.

Table 1
List of Low-Power Wireless Area Network (LPWAN).

Technology	Standard Body	Data Rate (kbps)	Range (km)	Battery Lifetime
LoRa [39]	LoRa Alliance	50	Urban:2-5, Suburban:15	>10 years
NB-IoT [39]	3GPP	200	10-15	>10 years (with a 5Wh battery)
SIGFOX [39]	SIGFOX	<100bps	Urban:3-10 Rural:30-50	10 years (Depending no. of message sent)
INGENU [39]	INGENU	DL:624 UL:156	Urban 15	10-20 years
Dash7 [40]	ISO/IEC 18000-7	13, 55, 200 (16, 8, 4 channels)	1 - 2	Multi-years (Not Specify)

# 2.3. Low-power wireless area network (LPWAN)-based sensors

A list of key features of LPWAN technologies, including data rate, range, battery life, and applications, has been thoroughly reviewed in [39–51]. Table 1 compares these key features of LPWAN-based sensors commonly used in remote-based applications. From this table, Long Range (LoRa) technology is often used in the Internet of Things (IoT) due to its low power, low cost, and flexible interface with various sensors [40].

Several applications in forestry monitoring and management have been successfully deployed; some examples include assisting and tracking tourists inside the forest for tourism [42], animal tracking [43], geographical surveillance [44–46], impact on foliage [47], visual and image surveillance [48,49], fire monitoring and management [50], and peatland monitoring and management [51].

The performance metric used to measure the power of the received signal at the wireless receiver (also known as radio frequency, or RF) is the received signal strength indicator (RSSI) [52]. In LPWAN, the RSSI is commonly used to estimate the range between transmitter and receiver apart [53]. Often, the RSSI reading is analyzed to understand the relationship between distance and received signal strength [54–56]. In recent years, several works have reported on how the RSSI has been used as an essential modality in various algorithm strategies, including localization applications to track and estimate the object of interest, such as Trilateration [57–59], Vector Similarity Degree, Support Vector Machine (SVM), Kalman Filter (KF) [60], and Recurrent Neural Network [61].

LoRa RSSI is also susceptible to propagation effects like any other LPWAN. Studies have investigated the RF's behavior in the foliage environment [48], and its propagation characteristic [18,62–64]. The studies are essential to understanding the relationship between RF behavior and local vegetation indices. LoRa uses a modulation scheme for data transmission based on Data Rate (DR) and Spreading Factor (SF). These two parameters are important for the success of data transfer over a long distance. Under harsh environments, the most suitable pair combines the highest DR with the lowest SF, and the opposite setup applies for good LOS [19,65–67]. Some reviews of LoRa transmission performance with DR and SF pairs can be found in [63], healthcare in [66], and utility [67].

#### 2.4. LoRa propagation model

A recent study reported that the new development of LoRa, which operates in the 2.4 GHz band and outperforms other technologies in similar bands in terms of communication range [68]. The results reveal that the maximum communications distance is 74 m in an indoor office environment and 443 m in an urban-type outdoor environment. LoRa communications range was also tested in the Antarctic region [69].

The longest recorded range in line-of-sight (LOS) was 30 km using the LoRa 484 MHz and 868 MHz bands. In subsequent works, measurement campaigns and modeling work observed successful communication distances of 4 km and 1 km for LOS and densely forested terrain [64].

In addition, the propagation of LoRa in the Malaysian region has been experimentally validated at a field test. Reference [48] proposed an algorithm to overcome the limitations of the LoRa physical layer in image transmission. The work presents encrypted image data in hexadecimal format, followed by segmenting the file into packets upon transmitting and receiving data ranging from 1 km to 7 km in the mangrove forest. The study in [70] reported that the weather conditions (including solar radiation, humidity, temperature, and rain) in the Malaysia region do not affect the LoRa RSSI performance. Moreover, studies associated with LOS in the Malaysia region have been evaluated in [71]. The results conclude that local vegetation, as a result of the tropical climate, contributes to greater attenuation in LoRa performance. The studies in [70,71] highlight an apparent discrepancy, emphasizing the need to address the research gap through further localized LoRa performance studies in Malaysia.

#### 2.5. LoRa data rate/spreading factor pairs

A series of studies have investigated the SF setup for LoRa performance. A related study published in 2018 looked at LoRa performance under various levels of interference, and a heavy path environment [19]. Upon transmission, the packet error rate (PER) in LoRa was measured via a three-parameter setup (spreading factor, bandwidth, and coding error rate). As it turns out, only SF has direct impacts on PER, which are grouped into two configurational space regions: the multipath-immune (or 0% PER) region for SF = 12-10 and the multi-path-sensitive (100%PER) region for SF = 9-7. In a healthcare study, a miniature LoRa was implanted into the human body to evaluate the low data rate transmission using LoRa backscatter signal as reported in [66]. Results demonstrated that the sensitivity and reliability of data transmission were better when using high SF (SF = 12) than lower SF (SF = 7). In addition, the high SF (SF = 12) setup used in the pilot study focuses on the design, implementation, optimization, and verification of smart meter systems using LoRa [67]. The high SF setup revealed the average relative error was below 3%, with all land-cover with LoRa signal despite strong signal attenuation.

#### 3. Signal transmission and propagation

This section is divided into two parts: the first part introduces the terminology of LoRa, RSSI, and SNR, while the second part explores the theory of Fresnel zone for wireless communication in space. The primary objective of this section is to provide readers with a clear understanding of the technical definitions used in Section 4 and to establish a foundation for the results presented in Section 5.

#### 3.1. RSSI and SNR

A simple relationship for radio circuit communication in free space can be portrayed using the ratio of power at the received antenna over the transmitter antenna, which can be written in (1) [72],

$$\frac{P_r}{P_t} = \frac{G_t G_r \lambda^2}{P_t (4\pi d)^2},\tag{1}$$

where  $P_r$  and  $P_t$  are the receiving power and transmitting power measured in mW,  $G_t$  and  $G_r$ , are the gain for transmitting and receiving antennas, respectively,  $\lambda$  is the wavelength in m,  $P_t$  are generalized path losses in mW, and d is the distance between two antennas in m.

Hence, the path loss for any communication can be defined as  $P_r$  over  $P_t$  ratio. The ratio is described logarithmically in units of dBm because the value is often very low. Rearranging (1), the  $P_r$  described in unit dBm given in (2) [72].

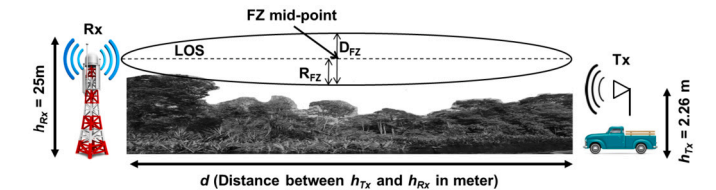


Fig. 2. Fresnel Zone illustration.

$$P_r[dBm] = 10 \cdot log_{10} \frac{P_t G_t G_r \lambda^2}{P_t (4\pi d)^2}$$
 (2)

Note that  $P_t$ ,  $G_t$ , and  $G_r$  are often expressed in dBm. Hence, it is appropriate to perform a unit conversion from mW to dBm given in (3).

$$P[dBm] = 10 \cdot log_{10} \left( \frac{P[mW]}{1[mW]} \right)$$

$$P[mW] = 10^{\frac{(P[dBm])}{10}}$$
(3)

A typical LPWAN communication is best represented by free-space path loss (FSPL), as given in (2) [73]. In a real-world environment, the communication signal experiences reflection from the ground, represented by the ground reflection coefficient (R) based on the height of the antenna transmitter (Tx) and receiver (Rx), respectively. For simplicity, this effect is known as the full two-ray model given in (4).

$$P_{r} = P_{t} \left(\frac{\lambda}{4\pi}\right)^{2} \left| \frac{\sqrt{G_{tr}}}{\sqrt{L_{-}^{2}}} + R \frac{\sqrt{G_{tr}}e^{-j\left(\frac{2\pi(\sqrt{L_{+}}) - (\sqrt{L_{-}})}{\lambda}\right)}}{L_{+}} \right|^{2}$$

$$L_{+} = d^{2} + (h_{t} + h_{r})^{2}$$

$$L_{-} = d^{2} - (h_{t} - h_{r})^{2}$$

$$G_{tr} = G_{t}G_{r},$$
(4)

where  $h_t$  is the height of LoRa node (Tx) and  $h_r$ , is the height of LoRa gateway (Rx) antenna in meter,  $L_+$  is positive path-length,  $L_-$  is negative path-length,  $G_{tr}$  to represent antenna gain of  $G_t$  and  $G_r$ , respectively, and R constant given by (-1 represents perfect ground reflection, and 0 represents zero ground reflection) [74,75].

In free-space propagation, the background noise is accounted for by the signal-to-noise ratio (SNR). It measures the ratio between the desired received signal power level,  $P_{signal}$  to the power level of background noise,  $P_{noise}$ . SNR is often represented in the logarithmic decibel scale as many signals have a significant dynamic range, as given in (5). In the LoRa system environment, the SNR reading subject to SF is used, reflecting its ability for long-distance communication discussed in Section 4.

$$SNR_{dB} = 10 \log \frac{P_{signal}}{P_{noise}} \tag{5}$$

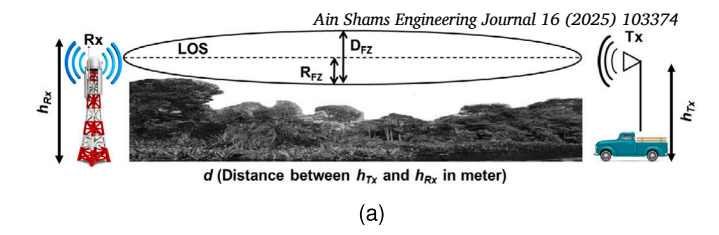
# 3.2. Fresnel zone at RMFR

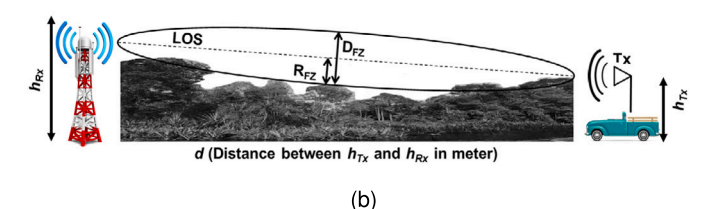
The diverse landscape at RMFR introduces additional communication losses between the Tx and Rx antennas. These obstacles appear in the so-called "Fresnel zone (FZ)" due to obstacles (e.g., palm oil trees, forest trees, and bushes), defined as a point-to-point network drawn in the shape of a cylindrical ellipse between Rx and Tx. A simple LOS point-to-point LoRa communications test environment is shown in Fig. 2 to portray the Fresnel Zone at RMFR.

The FZ mathematical expression given in (6) [48],

$$R_{FZ} = 8.656 \times \sqrt{\frac{d}{F}}$$

$$D_{FZ} = \sqrt{d_t^2 + R_{FZ}^2} + \sqrt{d_r^2 + R_{FZ}^2} - n\frac{\lambda}{2}$$
(6)





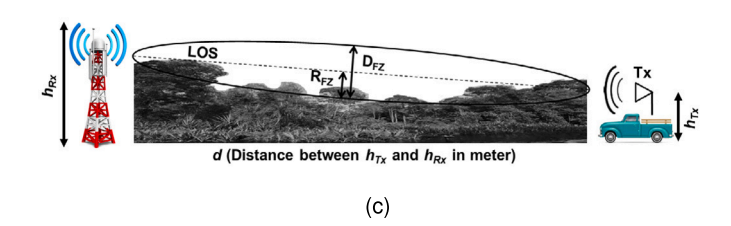


**Fig. 3.** Illustration of Fresnel zone (FZ) point-to-point LoRa communication at RMFR a) Fresnel zone 1: ideal-LOS, b) Fresnel zone 2: near-LOS, c) Fresnel zone 3: non-LOS.

 $R_{FZ}$  is the radius of FZ,  $d_t$  and  $d_r$  is the distance between Tx and Rx reference to FZ mid-point calculated using (7), F is the frequency of LoRa, and n denoted as n-th FZ.

With reference to (7), FZ mid-point can be calculated by using (6),

$$FZ_{m} = \frac{h_{Tx} + h_{Rx}}{2}$$

$$FZ_{ave} = \frac{h_{Ht} + h_{Lt}}{2}$$
(7)

where  $FZ_m$  is FZ mid-point,  $h_{Tx}$  and  $h_{Rx}$  is height of Tx and Rx respectively,  $FZ_{ave}$  is average obstacle height,  $h_{Ht}$  and  $h_{Lt}$  referring to a highest and lowest obstacle (e.g. palm oil tree, forest tree, and bushes) respectively.

The space between Tx and Rx needs to be kept as clear as possible to maximize communication efficiency. In that case, maximum obstruction is maintained at 40%, the recommended obstacle is 20% or less [76]. Due to several FZ at RMFR, it can be grouped into three categories as illustrated in Fig. 3, referred to as Fresnel zone 1 (FZ1) for ideal-LOS, Fresnel zone 2 (FZ2) for near-LOS, and Fresnel zone 3 (FZ3) for non-LOS.

At this point, three FZ categories, as illustrated in Fig. 3 can be denoted via the approximate function given in (8) to portray the terrain and landscape at RMFR [77]. As given in (4), received power  $P_r$  varies with d and  $h_{Tx}$  and  $h_{Rx}$ , respectively. Thus, FZ free zone can be calculated as given in (9).

$$P_r = \begin{cases} \text{Fresnel Zone 1} & \text{if } d < h_{Tx}, \\ \text{Fresnel Zone 2} & \text{if } h_{Rx} \le d \le h_{Tx}, \\ \text{Fresnel Zone 3} & \text{if } d > h_{Tx} \end{cases} \tag{8}$$

$$FZ_{\%} = \left(100 - \frac{FZ_{cr}}{D_{FZ}} \times 100\%\right)$$

$$FZ_{cr} = FZ_{ave} - FZ_{ch}$$

$$FZ_{ch} = FZ_m - R_{FZ}$$
(9)

where  $FZ_{\%}$  is the available FZ,  $FZ_{cr}$  is distance of the obstacle which crossed the  $FZ_{ch}$ , and  $FZ_{ch}$  is the FZ center height.

The most apparent feature of LoRa is its capability to communicate over a long distance. To achieve this, the data that is represented as a symbol is transmitted and received using the chirp spread spectrum (CSS) technique, multiplied with the spreading code or chip sequence known as the SF [78]. The duration of a chirp signal,  $T_s$  is defined as a function of bandwidth (BW), and SF as given in (10) [19].

$$T_s = \frac{2^{SF}}{BW} \tag{10}$$

The available BW are 125 kHz, 250 kHz, and 500 kHz, with the smallest BW contributing to the highest sensitivity for long transmission. Such a modulation design helps the receiver maintain the received data even at a further distance.

It is worth noting that the lowest DR with a higher SF provides ample time on-air with less data transmitted per unit of time, making it suitable for harsher terrain and landscapes. Under the near-LOS environment, the highest DR with the lowest SF and shortest time on-air allowed more data to be transmitted per unit time, becoming an appropriate setup [19]. The sensitivity level of the receiver relies on the following formula [79]:

$$Sensitivity = -170 + log_{10}(BW) + NF + SNR$$
(11)

where NF is the fixed noise floor for a given hardware, and SNR is the signal-to-noise ratio. SNR is inversely proportional to SF. Consequently, as BW decreases and SF increases, sensitivity decreases, allowing communication distance to increase. The DR formula is given in (12) [79], and the list of DR/SF pairs is listed in Table 6.

$$DR = SF \times \frac{BW}{2^{SF}} \cdot \frac{4}{4 + CR}$$

$$CR = 1.2.3 \text{ or } 4$$
(12)

# 4. Data collection and experimental setup

The Malaysian peatland forest is estimated at 1.54 Mha, with 70% of these forests found in Sarawak, situated in the northern part of Borneo Island; less than 20% in Peninsular Malaysia, and the remainder in Sabah [80], next to Sarawak. In terms of composition, Malaysian peatland is similar to Indonesian peatland in that it is acidic, waterlogged (up to a 25 m thick layer), and rich in phenol compounds [81]. Despite numerous studies on Malaysian peatland so far, only a few monitoring and management activities have been carried out in recent years, such as in [82–85]. To manage fire risk, after work, a system called FDRS has been adopted from the Canadian Forest Fire Danger Rating System for combating fire events in 1998 [15]. FDRS is a system that monitors forest fire risk and supplies information that assists in fire management. The system assists and guides policymakers in developing actions to protect life, property, and the environment.

The RMFR is a peatland forest reserve, in the district of Kuala Selangor, in the state of Selangor, Malaysia (GPS Coordinates: 3°27'57.42"N, 101°26'29.69"E) as shown in Fig. 1 was chosen for experiment site. Previously, this peatland belonged to the state government and had been extensively logged since the 1950s before it was gazetted to be reserved in 1990. Since then, a series of rehabilitation processes have been conducted to restore its landscape and return it to its original state. However, in 2014, RMFR suffered a massive fire that destroyed a large part of the peatland forest. The burned areas are dominated mainly by species, such as *Macaranga spp.* and *Imperata cylindrica*. The consequence is inevitable, with the loss of high-value timber, herbs, habitat, and wildlife [86].

Two sets of LoRa sensor nodes were set up in the IoT system (refer Fig. 7), linked to the network infrastructure of the LTE LoRaWAN gateway, powered by a solar panel backed by a deep cycle battery. The other instruments were a weather station and CCTV for security observations, as shown in Fig. 4.

A 5 dBi dipole antenna was installed on the top of the tower, located south of the RMFR peatland forest. Presently, the two LoRa nodes mea-



Fig. 4. Aeriel view of LoRaWAN facilities and infrastructure at RMFR.

sure the GWL under the peat soil surface, developing an improved FRDS for RMFR peatland forest.

#### 4.1. Land-covers characteristic

The decision to select the land-covers was made to cover diverse landscapes caused by post-fire events after seeking advice from the Institute of Tropical and Forestry and Forest Product (INTROP), Universiti Putra Malaysia (UPM), and Selangor State Forestry Department (JPNS). Due to differences in forest canopy height, different land use types emerge at the RMFR, including grassland, light bushes, and dense palm oil tree plantations. As a result, each land-cover has a distinct FZ profile, worthwhile to study. Ideally, there should be three FZ categories labeled at each land-cover as described in Section 3.2. However, none of these land-cover fall under FZ1, because peatland is prone to regenerating cycles. After a few years, when fire invades the area, new vegetation will grow, which is common in peatland after it has caught fire. Because of this, the region between the transmitter and receiver no longer has an ideal-LOS.

In this paper, land-cover that the receiver can still see from the transmitter was labeled as FZ2, although there is a forest canopy in between. While areas in which the region between receiver and transmitter was completely blocked by forest canopy were labeled as FZ3. Hence, seven land-covers have been chosen for the RF measurement campaign as shown in Fig. 5. The land-covers consist of oil palm, forest trees, bushes, disused sand mines, or a combination of those vegetation types, as reported in [87]. The description of land-covers is depicted in Table 2.

#### 4.2. Fresnel zone model at RMFR

A simple model of  $FZ_{\%}$  at RMFR was calculated in this paper using (9) to guide us in interpreting the results in Section 5. A simple model of  $FZ_{\%}$  consists of two types of plants: a thick and solid trunk tree (representing oil palm and forest trees) and a shrub (representing bushes), as shown in Fig. 6.

The tree height estimation is taken from the observations of the Institute of Tropical and Forestry and Forest Product (INTROP) UPM and the Selangor State Forestry Department (JPNS) at RMFR. As the height of plants at RMFR varies depending on its land-covers, the estimation for maximum and minimum height was considered in the equation, with heights for Rx and Tx equal to 25 m and 2.26 m, respectively.

- In the thick and solid trunk tree area, the maximum and minimum heights are 10 m and 4 m, respectively.
- In the shrub area, the maximum and minimum heights are 7 m and 3 m, respectively.

The calculated  $FZ_\%$  for thick and solid trunk trees and shrubs at RMFR are tabulated in Table 3 and Table 4, respectively. Seven LoRa



Fig. 5. Location of LoRa RF measurement campaign at RMFR.

**Table 2**Land-covers description (Refer Fig. 5 for each land-covers pictures.

Land-Covers	Distance (km)	Fresnel Zone	Land-Cover Description
1	0.1	FZ2	Regeneration peatland area. Light bushes vegetation with a height range from 3 m to 7 m. South from gateway tower. GPS coordinate: 3.4461458, 101.4421353
2	1.1	FZ3	Replanting peatland area.  Dense forest tree vegetation with height range 5 m to 7 m  Southwest from gateway tower.  GPS coordinate: 3.4574351, 101.4363652
3	1.3	FZ3	Palm oil plantation.  Dense palm oil tree plantation with height range 4 m to 6 m.  Northeast from gateway tower.  GPS coordinate: 3.4769299, 101.44559924
4	2.3	FZ2	Regeneration peatland area. Surrounded by bushes with height range 3 m to 7 m. Southwest from gateway tower. GPS coordinate: 3.4464222,101.4342872
5	3	FZ2	Natural peatland area.  Dense forest tree vegetation with height range 7 m to 10 m.  Southwest from gateway tower.  GPS coordinate: 3.4414102, 101.4303454
6	4	FZ2	Regeneration peatland area. Moderate bushes vegetation with height range 3 m to 7 m. Southwest from gateway tower. GPS coordinate: 3.431551, 101.4247281
7	5	FZ2	Natural peatland area.  Dense bushes vegetation with height range 4 m to 5 m.  Southwest from gateway tower.  GPS coordinate: 3.4254318, 101.422008

Channels (Ch) were used to calculate the  $FZ_{\%}$ , at those frequencies approved by the Malaysian Communications and Multimedia Commission (MCMC), the national communications regulatory agency. The land-covers nearest to Rx offers the largest  $FZ_{\%}$ , and this reading subsequently degrades as the Tx moves away from the Rx locations.

From Fig. 6, the  $FZ_{\%}$  for shrubs is generally higher than the  $FZ_{\%}$  for thick and solid trunk trees at the same distance. Hence, the transmission path loss and  $FZ_{\%}$  contribute to the LoRa RF signal quality and data transmission performance;  $FZ_{\%}$  is larger in shrub areas than in large trees and forest areas. Moreover, there is no or little degradation of  $FZ_{\%}$  at different Ch (frequency) on the same land-cover.

As a result, reduced  $FZ_\%$ , contributes to higher path loss, resulting in lower RSSI, SNR, and FT rate within the RMFR presented in Section 5 and discussed in Section 6. After all, none of these land-covers for data collection fall into FZ1 (referring to Fig. 5 and Table 2).

# 4.3. Experimental methodology

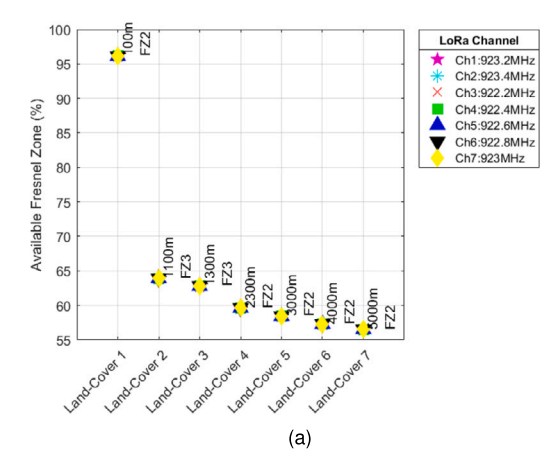
The experimental setup consists of a LoRa node (model RHF3M076), a laptop computer, an external antenna, and a GPS logger, as shown in Fig. 7. The LoRa node must be registered in an existing LTE LoRaWAN infrastructure before data can be pushed into the cloud server via an

Table 3 The Fresnel Zone,  $FZ_{\%}$ , as given in (9), was calculated at RMFR for shrub land-cover.

Land- Covers	Available Fresnel Zone, $FZ_{\%}$ Channel, Ch (MHz)						
	Ch1 923.2	Ch2 923.4	Ch3 922.2	Ch4 922.4	Ch5 922.6	Ch6 922.8	Ch7 923
1	201.46	201.48	201.38	201.39	201.41	201.43	201.44
2	95.66	95.67	95.64	95.64	95.65	95.65	95.66
3	92.00	92.01	91.98	91.99	91.99	91.99	92.00
4	81.58	81.58	81.56	81.56	81.57	81.57	81.57
5	77.65	77.65	77.63	77.64	77.64	77.64	77.65
6	73.94	73.95	73.93	73.93	73.94	73.94	73.94
7	71.42	71.42	71.40	71.41	71.41	71.41	71.41

**Table 4** The Fresnel Zone,  $FZ_{\%}$ , as given in (9), was calculated at RMFR for thick and solid trunk trees land-cover.

Land- Covers/	Available Fresnel Zone, $FZ_{\%}$ Channel, Ch (MHz)						
	Ch1 923.2	Ch2 923.4	Ch3 922.2	Ch4 922.4	Ch5 922.6	Ch6 922.8	Ch7 923
1	157.58	157.59	157.52	157.54	157.55	157.56	157.57
2	82.43	82.44	82.42	82.42	82.42	82.43	82.43
3	79.83	79.84	79.82	79.82	79.82	79.83	79.83
4	72.43	72.43	72.42	72.42	72.42	72.42	72.43
5	69.64	69.64	69.63	69.63	69.63	69.63	69.64
6	67.01	67.01	67.00	67.00	67.00	67.00	67.00
7	65.21	65.21	65.20	65.20	65.21	65.21	65.21



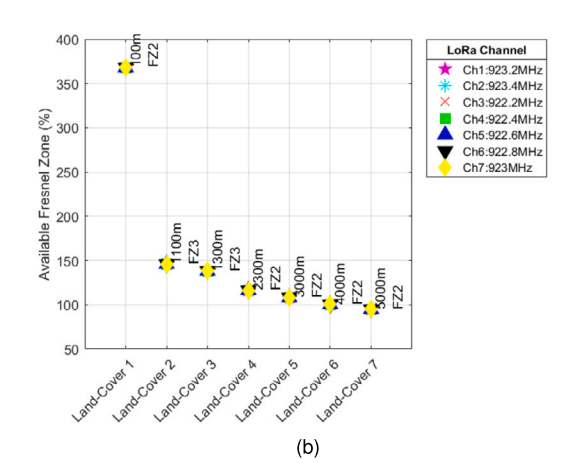


**Fig. 6.** Plot of the calculated available Fresnel Zone,  $FZ_{\%}$ , for shrub, thick and solid trunk trees land-cover at RMFR, based on (9). a) Shrub plants, b) Solid and thick plants.

Table 5 LoRa system setup.

LoRa parameter	Parameter value
Activation method	OTAA
Gateway transmit power	26 dBm
Node transmit power	14 dBm
Bandwidth	125 kHz
Packet size	13 bytes
End device output power	14 dBm
End device antenna gain	5 dBi
Gateway height (Rx)	25 meter
Node height (Tx)	2.26 m
LoRa frequency	Tabulated in Table 6

LTE network. The LoRa node is enclosed in a rugged case suitable for outdoor use. An off-road four-wheel drive vehicle was used since the road and terrain along the land-covers can be harsh, such as gravel, sand, and mud. An external antenna was attached to the LoRa node and placed on top of the vehicle to maximize signal reception. Data collection was entirely controlled and monitored on the laptop computer via a Python script, so individual execution and action could be taken immediately to address any problem. The setup is illustrated in Fig. 7.

## 4.4. LoRa RF setup

The LoRa system setup is summarized in Table 5. As presented in Table 6, seven channels (Ch) were tested. This frequency spectrum is reserved for the Malaysian region and approved by the Malaysian Communications and Multimedia Commission (MCMC) [88]. The effect of LoRa frequency on  $FZ_{\%}$ , which reflects the RSSI, SNR, and file transfer success rate, will be further described in Section 5.

Six DR/SF pairs for the Malaysia region were used [78], with ten file transfer (FT) attempts for a file size of 13 bytes; this is summarized in Table 7. For monitoring purposes, each FT transfer sequence is labeled as  $FT_n$ , where n (n = 1,2,3,...,10) represents the sequence of FT. The bandwidth (BW) is fixed, at 125 kHz and was used throughout the measurement campaign.

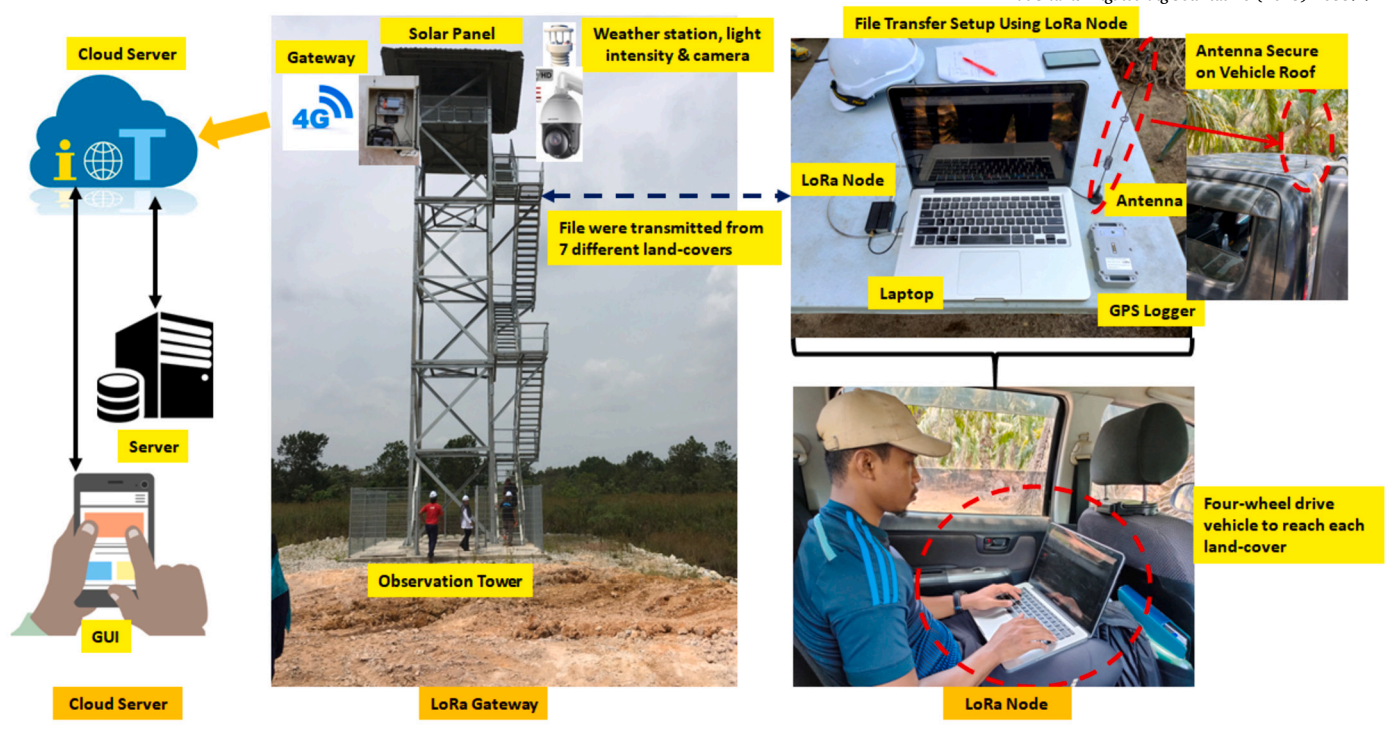


Fig. 7. Experimental setup for RF measurement campaign at RMFR.

Table 6
LoRa channels and frequency.

LoRa Channel (Ch)	Frequency (MHz)
1	923.2
2	923.4
3	922.2
4	922.4
5	922.6
6	922.8
7	923.0

**Table 7**LoRa RF Parameter and File Transfer Setup.

Data Rate (DR)	Spreading Factor (SF) /Bandwidth (kHz)	File Transfer Attempt (FT)	File Size (byte)
DR0	12/125	10	13
DR1	11/125	10	13
DR2	10/125	10	13
DR3	9/125	10	13
DR4	8/125	10	13
DR5	7/125	10	13

For easier notation, data collection in this paper included RSSI, SNR, and FT, which were implemented using Python scripts, summarized in Algorithm 1. The script is initiated using a single channel, followed by a DR/SF pair before the FT process. The routine is repeated for the subsequent channels at all land-covers. Then, the FT success rate,  $FT_{\%}$  is calculated and given in (13) at each land-cover.

$$FT_{\%} = \frac{FT_s}{FT_T} \times 100\%$$

$$i = 1, 2, 3, ..., 10$$
(13)

where  $FT_s$  is file transfer successfully received, i is file transfer count, and  $FT_T$  is total file transfer transmitted for individual pair DR/SF.

#### Algorithm 1 Classification Process Algorithm.

**Input:** Set up the LoRa RF with a bandwidth of 125 kHz, using a combination of 7 channels (Ch) and 6 DR/SF pairs as shown in Table 7. Transmit 10 files per setup.

Output: Record the LoRa RSSI, SNR, and successful file transmissions at different land-cover types, and save the data into CSV format for post-processing in MATLAB. Store the data as time-series in the CSV file format.

Initialisation:

```
1: LOOP Process
 2: for ch = 1 to 7 do
      while condition DR/SF = \text{True do}
 3:
         if FT_i \leq 10 then
 4:
            FT_i = FT_i + 1
 5:
         else \{FT_i > 10\}
 6:
 7:
           count FTs
           Record the RSSI and SNR readings.
 8:
 9:
         Proceed with the next DR/SF pair.
10:
       end while
11:
12:
      Break save the data.
13: end for
14: return
```

#### 5. Results

This section divides the results into two sub-sections: i) RSSI and SNR were collected with distance (land-covers), and ii)  $FT_{\%}$  was calculated using DR/SF pairs. First, RSSI and SNR readings (all channels) were averaged and plotted against land-covers. The  $FT_{\%}$  trend at each land-cover type was then plotted against DR and SF. The Rx and Tx heights were maintained at 25 m and 2.26 m, respectively.

# 5.1. RSSI and SNR reading versus distance at RMFR

The theoretical  $FZ_{\%}$  plotted in Fig. 6 revealed an insight into how the RSSI and SNR from data collection at RMFR will appear. As presented in (1) and (5), RSSI reading tends to degrade with the Tx-Rx sep-

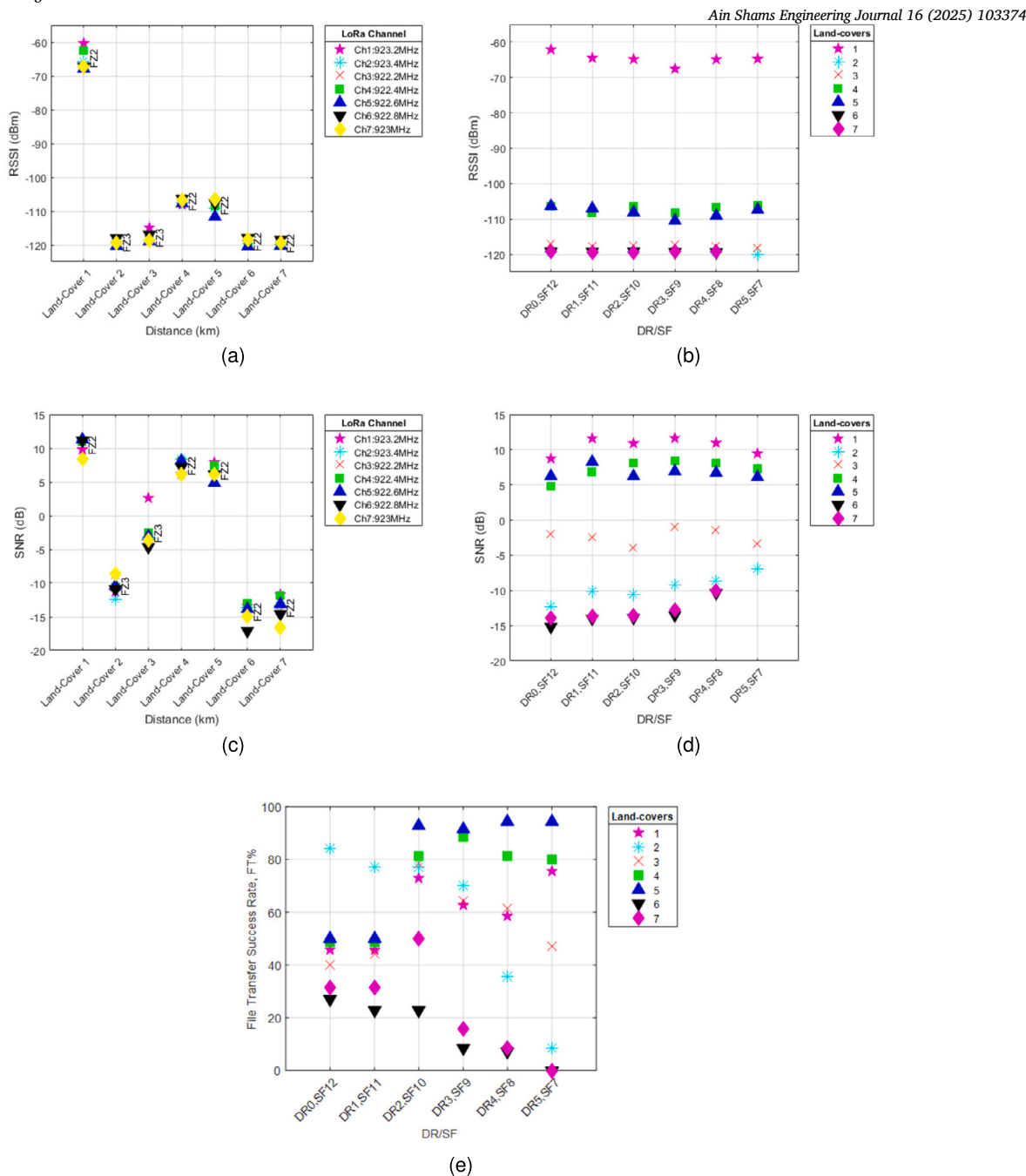


Fig. 8. The average plotted trend for LoRa RF numerical value versus land-covers, and versus DR/SF pairs. The combination of path loss and  $FZ_{\%}$  largely contributes to the degradation of both RSSI and SNR reading as discussed in Section 3. To ensure successful data transmission, rugged vegetation caused by forest canopy often required a combination of the lowest DR (DR0), highest SF (SF12), and a narrow bandwidth setup, whereas the opposite setup for surrounding with good LOS was required. [48]. The overall FT success rate trend revealed, the best FT success rate was achieved using a lower DR/higher SF pair at near-LOS (FZ2), and a higher DR/lower SF pair at non-LOS (FZ3) respectively at land-covers within RMFR as shown in Fig. 8e. a) Average RSSI vs land-covers, b) Average RSSI vs DR/SF pairs, c) Average SNR vs land-covers, d) Average SNR vs DR/SF pairs, e) File transfer success rate,  $FT_{\%}$  group into respective DR/SF pairs.

aration land-covers, d (height Tx and Rx are maintained in this work). Furthermore, blockage (referred to as  $FZ_{\%}$  factor) between Tx and Rx contributes to the signal losses. To characterize this event, we grouped the landscape and terrain at each land-cover given in (7).

The trend in Fig. 8a and Fig. 8c respectively, showed that the RSSI and SNR degrade with Tx-Rx distance due to path loss. Furthermore, as discussed in Section 3, the  $FZ_{\%}$  contributes significantly to the degradation of both RSSI and SNR. Other observations that can be derived from these plots are:

- Land-cover 1 obtained the best RSSI and SNR readings because it is closest to the gateway tower (Rx) despite being surrounded by light vegetation.
- Due of the  $FZ_{\%}$  factor, land-covers 4 and 5 have higher RSSI and SNR readings than land-covers 2 and 3.
- Land-cover 2 and 3, surrounded by dense oil palm trees and thick solid trunk trees, respectively, scored lower RSSI and SNR readings than land-cover 4 and 5.
- Land-cover 6 and 7 (near LOS) obtained among the lowest RSSI and SNR readings due to  $FZ_{\%}$  and distance factors.

**Table 8**Average RSSI at each land-cover.

Land- Covers	Available RSSI Reading (dBm) Channel, Ch (MHz)						
	Ch1 923.2	Ch2 923.4	Ch3 922.2	Ch4 922.4	Ch5 922.6	Ch6 922.8	Ch7 923
1	-60.35	-65.77	-62.64	-62.64	-67.88	-67.28	-67.16
2	-119.50	-119.58	-118.78	-119.41	-120.31	-118.05	-119.30
3	-114.90	-118.59	-117.66	-118.51	-118.93	-117.00	-118.64
4	-108.08	-107.48	-106.42	-107.04	-107.72	-106.37	-106.69
5	-107.04	-109.19	-107.73	-108.41	-111.68	-107.60	-106.52
6	-119.33	-119.71	-118.54	-119.45	-120.50	-118.00	-118.50
7	-119.84	-119.90	-119.10	-119.33	-120.25	-118.45	-119.50

**Table 9**Average SNR at each land-cover.

Land- Covers	Available SNR Reading (dB) Channel, Ch (MHz)						
	Ch1 923.2	Ch2 923.4	Ch3 922.2	Ch4 922.4	Ch5 922.6	Ch6 922.8	Ch7 923
1	9.81	11.15	10.93	10.97	11.30	11.15	8.40
2	-11.31	-12.48	-8.81	-10.64	-10.40	-10.92	-8.59
3	2.6122	-3.12	-4.05	-2.52	-3.07	-4.66	-3.68
4	6.17	8.39	7.94	8.04	8.13	7.21	6.11
5	7.90	6.65	7.47	7.47	4.85	6.11	6.13
6	-13.40	-13.62	-13.55	-13.08	-13.85	-17.10	-14.95
7	-11.70	-13.37	-14.27	-11.91	-13.10	-14.60	-16.60

• Hence, we concluded land-cover 1, 4, 5, 6, and 7, and land-cover 2 and 3 fall into FZ2 and FZ3, respectively.

The plots of the trend shown in Fig. 8a and Fig. 8c are tabulated in Table 8 and 9, respectively, for easier numerical comparison. Hence, we can verify that an increased distance between Tx and Rx introduced RF losses, as explained in Section 3. Therefore, we could hypothesize that the combination of path loss characteristics and FZ largely contributes to the observed RSSI and SNR result trend at RMFR.

#### 5.2. File transfer success rate based on DR/SF pairs

The DR/SF pairs and bandwidth determine the transmission and receiving LoRa system performance in various environments. The rugged vegetation necessitated a combination of the lowest DR (DR0) and highest SF (SF12) and a narrow bandwidth configuration, as well as the opposite configuration for surrounding areas with good LOS [19]. Since the land-covers at RMFR vary, it is better to study and analyze FT success rates by flagging them according to DR/SF pairs.

At this stage, we managed  $FT_{\%}$  results by categorizing FT status based on the pair of DR and SF profiles. From (13), the total FT samples equal 420 at each land-cover, but the actual FT sample is expected to be lower because some of the FT failed upon data collection. Table 10 exhibits the best FT success rate based on DR/SF pairs at each land use. Based on Table 10, the following points could be observed for  $FT_{\%}$  at land-cover within RMFR:

- At land-cover 1, closest to the Rx, the highest FT success rate is achieved using the DR5/SF7 pair.
- At land-cover 7, the farthest point from the Rx, a slightly lower DR/SF pair is used (DR2/SF10).
- At land-cover 2 and 6, the DRO/SF12 pair is the most suitable pair, as the vegetation of the land-cover was harsher than the other landcover.

Fig. 8b and Fig. 8d respectively, show the plots of RSSI and SNR readings received by the LoRa gateway (Rx) from the LoRa node (Tx) against various DR/SF pairs. The modulation scheme of LoRa strongly

**Table 10** Best file transfer success rate,  $FT_{\%}$  based on DR/SF pairs.

Land- Covers	Data Rate (DR)	Spreading Factor (SF)	Average RSSI (dBm)	Average SNR (dB)	FT Success Rate(%)
1	5	7	-64.75	9.45	75.71
2	0	12	-119.36	-12.29	84.29
3	2	10	-117.67	-3.97	78.27
4	3	9	-108.32	8.45	88.57
5	4	8	-108.32	8.45	94.29
6	0	12	-119.21	-15.16	27.14
7	2	10	-119.40	-13.60	50.00

depends on DR/SF pairs, as described in Section 3 given in (12). From this plot, the following conclusion could be drawn:

- Land-cover 3 and 4 have RSSI and SNR higher than land-cover 2 and 3, mainly due to the FZ factor, as described in (8).
- The RSSI and SNR readings of LoRa are related to the path loss characteristics and FZ when they are grouped by DR/SF pairs.

The overall FT success rate trend is portrayed in Fig. 8e, and it shows that the land-covers of near-LOS within RMFR achieved the best FT success rate using a lower DR and higher SF pair. In contrast, for land-covers under non-LOS within RMFR, a higher DR and lower SF pair is more appropriate. Under these circumstances, the DR5/SF7 pair failed to receive the data, mainly due to the longer distances and harsh terrain and land-scape within RMFR.

## 6. Discussion

Results in Section 5 demonstrate that each land-cover achieved the highest  $FT_{\%}$  by utilizing a dedicated pair of DR/SF, as indicated in Table 6. Based on these findings, we propose that LoRa sensor nodes within the RMFR be configured with specific DR/SF pairs to optimize transmission performance, as illustrated in Fig. 9. For instance, the DR5/SF7 pair is well-suited for good LOS conditions, as observed in land-cover 1. Conversely, in areas with dense vegetation, such as land-cover 2, the DR0/SF12 pair is ideal for non-LOS scenarios.

We have observed that the positioning of the gateway tower antenna, as depicted in Fig. 4, potentially impacts the quality of  $FT_{\%}$  within the land-cover areas of RMFR. By referring to Fig. 5, we note that only land-cover 1 and 3 have the gateway antenna facing away from the LoRa test node situated at the respective land-covers. The  $FT_{\%}$  trend, particularly for land-covers 1 and 3, will be discussed in the following points:

•  $FT_{\%}$  at land-cover 1 scores lower than other land-cover despite being closer and having the best RSSI and SNR readings (refer Table 7 and 8 respectively) compared to other land-cover locations.

Light vegetation areas (DR5/SF7) are suitable for LOS communications. Dense vegetation areas (DR0/SF12) are suited for



Fig. 9. Visual representation of RMFR land-cover types with corresponding LoRa performance parameters (DR/SF pairs setup), based on experimental results reported in this paper. Light vegetation areas (DR5/SF7) are shown to be suitable for LOS communications, while dense vegetation areas (DR0/SF12) are suited for non-LOS communications

**Table 11**Correlation Coefficient Score of LoRa RF Parameter against Ambient Temperature.

Land- Covers	Average Temperature (°C)	Correlation Coefficient (RSSI vs °C)	Correlation Coefficient (SNR vs °C)
1	29.22	-0.4776	-0.1506
2	30.70	0.1276	0.1849
3	32.01	0.1220	0.2641
4	32.46	-0.1146	-0.0997
5	27.73	-0.0826	-0.0291
6	23.93	0.2796	-0.3349
7	24.32	0.3542	-0.3243

- Land-cover 3  $FT_{\%}$  scores lower than land-cover 2, despite having slightly higher  $FZ_{\%}$  as shown in Fig. 6.
- The cone-shaped roof of the gateway tower where the antenna is attached might have introduced additional blockage and interference between Tx and Rx, which results in higher failed file transfers for land-cover 1 and 3. This is shown in Fig. 4.

In evaluating the performance of  $FT_\%$  at different land-cover areas within RMFR, it is beneficial to group them based on DR/SF pairs. This approach has been validated and extensively investigated in recent studies [20,21], as supported by the  $FT_\%$  results presented in Section 5. Additionally, we analyzed the correlation between LoRa RF performance and the average RSSI and SNR readings in relation to ambient temperature. However, none of the temperature readings exhibited a strong correlation coefficient, as indicated in Table 11. Therefore, the ambient temperature factor does not significantly influence the performance of LoRa RF in the land-cover areas within RMFR.

Seamless data transmission from LoRa in the land-cover areas within RMFR is crucial to ensuring that data recorded by the sensor nodes are successfully transmitted and stored in the cloud. This reliable data can then be utilized to feed the FDRS prediction model, specifically designed for the peatland forest in RMFR, to enhance the accuracy of the peatland forest fire prediction. Furthermore, the following associated works are planned for future research:

# communications.

non-LOS

Key insights:

- Vegetation density varies:
  i. The DR decreases and
  the SF increases from
  light to dense.
- ii. The DR increases and the SF decreases from light to dense

#### DR/SF Optimization Framework:

 This visual representation serves as a valuable reference, highlighting its applicability to other peatland ecosystems and inspiring adaptations for similar environments.

- To conduct a measurement campaign in other RMFR land-covers in order to collect LoRa data. This is important to obtain insights on how LoRa RF will behave in the thick peatland forest ecosystem.
- 2) To raise the LoRa gateway antenna higher to maximize the reception signal between Tx and Rx within the RMFR peatland forest.
- Tuning the CR provides insight into the LoRa end-to-end communications performance, such as data rate, error correction capacity, and range factor [89].
- 4) To develop an improved FDRS prediction model for RMFR by combining satellite images of topography and land-covers at RMFR with in-situ data from a LoRa sensor node.

While the main focus of this paper is studying the optimal DR/SF pairs for reliable data transmission using LoRa in peat swamp forests in Malaysia, the utilization of remote-based technology aligns with the keywords used in the methodology by S. Monteverde et al. in their work on 'management and rehabilitation of peatland' [29]. This paper contributes to identifying gaps in the existing literature (discussed in Section 1) and aligns with ongoing efforts in peatland restoration and management. The implementation of the LoRa system has the potential to complement and enhance peatland forest management, as discussed in Section 2. In Section 3, a comprehensive technical description of the use of LoRa has been provided, offering a clear understanding of the technical definitions used to explain the methodology. LoRa operates under a spectrum reserved internationally for industrial, scientific, and medical (ISM) use and is widely used for research and scientific purposes, without any financial commitment required for spectrum licensing. Combining the keywords of lower operating costs, lower power consumption, and remote capability, the study presented in this paper is expected to significantly contribute to reducing financial commitments in efforts to restore and manage peatland forests [30].

# 7. Conclusion

This study investigated the optimal DR/SF configurations for reliable LoRa data transmission across different land-cover types within RMFR. The analysis evaluated the file transfer success rate (FT%) across six Data Rate (DR) and Spreading Factor (SF) values, identifying DR/SF pairings that maximize transmission reliability. These configurations en-

able consistent data collection within RMFR's peatland forest, supporting the development of an improved Fire Danger Rating System (FDRS). Beyond RMFR, the proposed DR/SF model provides a practical reference for LoRa RF planning in other peatland forests across Peninsular Malaysia, such as those in Batu Enam, Jalan Pekan, and Penor/Kuantan District, Pahang. The findings offer valuable insights for local authorities, researchers, and stakeholders in mitigating peatland forest fires and ensuring the sustainability of communities reliant on peatland ecosystems. Furthermore, these results contribute to a broader understanding of LoRa RF deployment in complex environments. The proposed model and transmission guidelines could serve as a reference for optimizing LoRa-based monitoring in other peatland ecosystems, facilitating advancements in environmental surveillance, resource management, and ecological conservation.

#### CRediT authorship contribution statement

Nur Luqman Saleh: Writing – original draft, Investigation, Formal analysis, Data curation. Aduwati Sali: Writing – review & editing, Supervision, Funding acquisition. Liew Jiun Terng: Writing – review & editing. Sharifah Mumtazah Syed Ahmad Abdul Rahman: Writing – review & editing. Azizi Mohd Ali: Writing – review & editing, Validation, Methodology. Borhanuddin Mohd Ali: Writing – review & editing. Sheriza Mohd Razali: Writing – review & editing, Validation, Supervision. Ahmad Ainuddin Nuruddin: Writing – review & editing, Conceptualization. Nordin Ramli: Writing – review & editing.

#### **Declaration of competing interest**

The authors declare that they have no known competing financial interests or personal relationships that could have appeared to influence the work reported in this paper.

# Acknowledgement

The authors would like to acknowledge NICT Japan and ASEAN-IVO NAPC (Networked ASEAN Peatland Forests Communities, Grant NO UPM - NICT 6380024-10801), NET-PEAT: Networked ASEAN Peatland Communities for Transboundary Haze Alert, Asia Pacific Telecommunity (APT), International Collaborative Research – Government of Japan, IGNITE - Interference Modelling for 5G and FSS Coexistence at mmWave with Climate Change Considerations in the Tropical Region (FRGS/1/2021/TK0/UPM/01/1, File No.: 03-01-21-2375FR. Vot No.: 5540509), and BIDANET: Parametric Big Data Analytics over Wireless Networks (UPM.RMC.800-3/3/1/GPB/2021/9696300, Vot No.: 9696300) for funding this project, Selangor State Forestry Department (JPNS) for permission to deploy the IoT system, MetMalaysia, LORANET Technologies and Global Environment Centre (GEC) for valuable feedback and validation of peatland data.

## References

- Joosten H. Peatlands, climate change mitigation and biodiversity conservation. Nordic council of ministers. 2015.
- [2] International W. A quick scan of peatlands in Malaysia. Tech. Rep.. Petaling Jaya, Malaysia: Wetlands International Malaysia; 2010.
- [3] Page SE, Hooijer A. In the line of fire: the peatlands of Southeast Asia. Philos Trans - R Soc B. Biol Sci Jun 2016;371:20150176.
- [4] Dohong A, Aziz AA, Dargusch P. A review of the drivers of tropical peatland degradation in South-East Asia. Land Use Policy Dec 2017;69:349–60.
- [5] Turetsky MR, Benscoter B, Page S, Rein G, van der Werf GR, Watts A. Global vulnerability of peatlands to fire and carbon loss. Nat Geosci Dec 2014;8:11–4.
- [6] Huijnen V, Wooster MJ, Kaiser JW, Gaveau DLA, Flemming J, Parrington M, et al. Fire carbon emissions over maritime Southeast Asia in 2015 largest since 1997. Sci Rep May 2016;6.
- [7] Spessa A, van der Werf G, Thonicke K, Dans JG, Lehsten V, Fisher R, et al. Modeling vegetation fires and fire emissions. In: Goldammer JG, editor. Vegetation fires and global change? Challenges for concerted international action. A white paper directed to the United Nations and international organizations; August 2013. p. 181–207.

- [8] Saputra E, Hartmann T, Zoomers A, Spit T. Fighting the ignorance: public authorities' and land users' responses to land subsidence in Indonesia. American Journal of Climate Change 2017;06(01):1–21.
- [9] Uda SK, Hein L, Atmoko D. Assessing the health impacts of peatland fires: a case study for Central Kalimantan, Indonesia. Environ Sci Pollut Res Aug 2019;26:31315-27.
- [10] Schrier-Uijl A, Silvius M, Parish F, Lim K, Rosediana S, Anshari G. Environmental and Social Impacts of Oil Palm Cultivation on Tropical Peat – A Scientific Review. 2013. Roundtable on Sustainable Palm Oil.
- [11] Page S, Hoscilo A, Langner A, Tansey K, Siegert F, Limin S, et al. Tropical peatland fires in Southeast Asia. In: Tropical fire ecology. Springer Berlin Heidelberg; 2009. p. 263–87.
- [12] Food and Agriculture Organization of the United Nations (FAO). Peatland mapping and monitoring – recommendations and technical overview. Rome, Italy: FAO; 2020.
- [13] Dargie GC, Lawson IT, Rayden TJ, Miles L, Mitchard ETA, Page SE, et al. Congo basin peatlands: threats and conservation priorities. Mitig Adapt Strategies Glob Change Jan 2018;24:669–86.
- [14] Li L, Sali A, Liew JT, Saleh NL, Ahmad SMS, Ali AM, et al. Estimation of ground water level (GWL) for tropical peatland forest using machine learning. IEEE Access 2022;10:126180–7.
- [15] Canada NR. Forest cover and other forest resources of Canada: National forest inventory 1995. 1997. Accessed: 2024-10-10.
- [16] Nath TK, Dahalan MPB, Parish F, Rengasamy N. Local peoples' appreciation on and contribution to conservation of peatland swamp forests: experience from Peninsular Malaysia. Wetlands Aug 2017;37:1067–77.
- [17] ASEAN Secretariat, Global Environment Centre (GEC). APFP-SEAPeat key achievements booklet 2010-2015. Jakarta, Indonesia: ASEAN Secretariat and Global Environment Centre; 2015.
- [18] Paredes M, Bertoldo S, Carosso L, Lucianaz C, Marchetta E, Allegretti M, et al. Propagation measurements for a LoRa network in an urban environment. J Electromagn Waves Appl Sep 2019;33:2022–36.
- [19] Staniec K, Kowal M. LoRa performance under variable interference and heavymultipath conditions. Wirel Commun Mob Comput 2018;2018:1–9.
- [20] Chall RE, Lahoud S, Helou ME. LoRaWAN network: radio propagation models and performance evaluation in various environments in Lebanon. IEEE Internet Things J Apr 2019;6:2366–78.
- [21] Xu W, Kim JY, Huang W, Kanhere SS, Jha SK, Hu W. Measurement, characterization, and modeling of LoRa technology in multifloor buildings. IEEE Internet Things J Jan 2020:7:298–310.
- [22] Cecílio J, Ferreira PM, Casimiro A. Evaluation of LoRa technology in flooding prevention scenarios. Sensors Jul 2020;20:4034.
- [23] Gaitan MG, d'Orey PM, Cecilio J, Rodrigues M, Santos PM, Pinto L, et al. Modeling LoRa communications in estuaries for IoT environmental monitoring systems. IEEE Sens J Nov 2022;22:21312–25.
- [24] Olasupo TO. Wireless communication modeling for the deployment of tiny IoT devices in rocky and mountainous environments. IEEE Sens Lett Jul 2019;3:1–4.
- [25] Myagmardulam B, Tadachika N, Takahashi K, Miura R, Ono F, Kagawa T, et al. Path loss prediction model development in a mountainous forest environment. IEEE Open J Commun Soc 2021;2:2494–501.
- [26] KeTSA. Forest fire analysis and forecasting in permanent forest reserve in Peninsular Malaysia. Big data analytics. 2022.
- [27] Barthelmes A, Ballhorn U, Couwenberg J. The high carbon stock science study: Independent report from the technical committee; consulting Study 5: Practical guidance on locating and delineating peatlands and other organic soils in the tropics. The high carbon stock study 2015. 2015.
- [28] Gumbricht T, Roman-Cuesta RM, Verchot L, Herold M, Wittmann F, House-holder E, et al. An expert system model for mapping tropical wetlands and peatlands reveals South America as the largest contributor. Glob Change Biol May 2017;23:3581–99.
- [29] Monteverde S, Healy M, O'Leary D, Daly E, Callery O. Management and rehabilitation of peatlands: the role of water chemistry, hydrology, policy, and emerging monitoring methods to ensure informed decision making. Ecol Inform Jul 2022;69:101638.
- [30] Reed M, Bonn A, Evans C, Glenk K, Hansjürgens B. Assessing and valuing peatland ecosystem services for sustainable management. Ecosystem Services Sep 2014;9:1–4.
- [31] Nations U. Report of the United Nations Environment Assembly of the United Nations Environment Programme: Fourth Session (Nairobi, 11-15 March 2019). 2019. UN.
- [32] Barchiesi S, Davies PE, Kulindwa KAA, Lei G, Del Río L, Martinez Ríos L. Implementing environmental flows with benefits for society and different wetland ecosystems in river systems. Ramsar Policy Brief 2018;(4).
- [33] Bourgeau-Chavez LL, Endres SL, Graham JA, Hribljan JA, Chimner RA, Lillieskov EA, et al. Mapping peatlands in boreal and tropical ecoregions. Elsevier; 2018. p. 24–44.
- [34] Millard K, Richardson M. Quantifying the relative contributions of vegetation and soil moisture conditions to polarimetric C-B and SAR response in a temperate peatland. Remote Sens Environ mar 2018;206:123–38.
- [35] Mandal D, Hosseini M, McNairn H, Kumar V, Bhattacharya A, Rao Y, et al. An investigation of inversion methodologies to retrieve the leaf area index of corn from C-Band SAR data. Int J Appl Earth Obs Geoinf oct 2019;82:101893.

- [36] Shofiana DA, Sitanggang IS. Confidence analysis of hotspot as peat forest fire indicator. J Phys Conf Ser Jan 2021;1751;012035.
- [37] Bechtold M, Schlaffer S, Tiemeyer B, Lannoy GD. Inferring water table depth dynamics from ENVISAT-ASAR C-Band backscatter over a range of peatlands from deeply-drained to natural conditions. Remote Sens Mar 2018;10:536
- [38] Anderson K, Bennie JJ, Milton EJ, Hughes PDM, Lindsay R, Meade R. Combining LiDAR and IKONOS data for eco-hydrological classification of an ombrotrophic peatland. J Environ Qual Jan 2010;39:260–73.
- [39] Popli S, Jha RK, Jain S. A survey on energy efficient narrowband Internet of things (NBIoT): architecture, application and challenges. IEEE Access 2019;7:16739–76.
- [40] Ayoub W, Samhat AE, Nouvel F, Mroue M, Prevotet J-C. Internet of mobile things: overview of LoRaWAN, DASH7, and NB-IoT in LPWANs standards and supported mobility. IEEE Commun Surv Tutor 2019;21(2):1561–81.
- [41] Ikpehai A, Adebisi B, Rabie KM, Anoh K, Ande RE, Hammoudeh M, et al. Low-power wide area network technologies for Internet-of-things: a comparative review. IEEE Internet Things J Apr 2019;6:2225–40.
- [42] Ferreira AE, Ortiz FM, de Almeida TT, Costa LHMK. A visitor assistance system based on LoRa for nature forest parks. Electronics Apr 2020;9:696.
- [43] Panicker JG, Azman M, Kashyap R. A LoRa wireless mesh network for wide-area animal tracking. In: 2019 IEEE international conference on electrical, computer and communication technologies (ICECCT). IEEE; Feb 2019.
- [44] Park S, Yun S, Kim H, Kwon R, Ganser J, Anthony S. Forestry monitoring system using LoRa and drone. In: Proceedings of the 8th international conference on web intelligence, mining and semantics. ACM; Jun 2018.
- [45] Sendra S, García L, Lloret J, Bosch I, Vega-Rodríguez R. LoRaWAN network for fire monitoring in rural environments. Electronics Mar 2020;9:531.
- [46] Zhu Y, Song J, Dong F. Applications of wireless sensor network in the agriculture environment monitoring. Proc Eng 2011;16:608–14.
- [47] Ahmad KA, Salleh MS, Segaran JD, Hashim FR. Impact of foliage on LoRa 433mhz propagation in tropical environment. In: AIP conference proceedings; 2018.
- [48] Jebril A, Sali A, Ismail A, Rasid M. Overcoming limitations of LoRa physical layer in image transmission. Sensors Sep 2018;18:3257.
- [49] Staikopoulos A, Kanakaris V, Papakostas GA. Image transmission via LoRa networks – a survey. In: 2020 IEEE 5th international conference on image, vision and computing (ICIVC). IEEE; Jul 2020.
- [50] Gaitan NC, Hojbota P. Forest fire detection system using LoRa technology. Int J Adv Comput Sci Appl 2020;11(5).
- [51] Sali A, Ali AM, Ali BM, Rahman SMSAA, Liew JT, Saleh NL, et al. Peatlands monitoring in Malaysia with IoT systems: preliminary experimental results. In: Advances in intelligent systems and computing. Springer International Publishing; 2021. p. 233–42.
- [52] Infrastructure L-EC, Layer MLP. IEEE standard for low-rate wireless networks. IEEE Stand 2015;2015:1–708.
- [53] Liu W, Kulin M, Kazaz T, Shahid A, Moerman I, Poorter ED. Wireless technology recognition based on RSSI distribution at sub-Nyquist sampling rate for constrained devices. Sensors Sep 2017;17:2081.
- [54] Obeidat H, Alabdullah AAS, Ali NT, Asif R, Obeidat O, Bin-Melha MSA, et al. Local average signal strength estimation for indoor multipath propagation. IEEE Access 2019;7:75166–76
- [55] Yamaoka Y, Hamasaki T, Kuramoto D. 2.4 GHz RF propagation measurements and modeling in a paddy field for a wireless sensor network. In: 2019 IEEE-APS topical conference on antennas and propagation in wireless communications (APWC). IEEE; Sep 2019.
- [56] Duda N, Weigel R, Koelpin A. Low-weight wireless sensor node with sensor-dataenhanced dual-frequency RSSI-based distance estimation. IEEE Trans Microw Theory Tech Oct 2020;68:4131–7.
- [57] Yang B, Guo L, Guo R, Zhao M, Zhao T. A novel trilateration algorithm for RSSI-based indoor localization. IEEE Sens J Jul 2020;20:8164–72.
- [58] Shi Y, Shi W, Liu X, Xiao X. An RSSI classification and tracing algorithm to improve trilateration-based positioning. Sensors Jul 2020;20:4244.
- [59] Minea M, Dumitrescu C, Costea IM, Chiva IC, Semenescu A. Developing a solution for mobility and distribution analysis based on bluetooth and artificial intelligence. Sensors Dec 2020;20:7327.
- [60] Shang F, Su W, Wang Q, Gao H, Fu Q. A location estimation algorithm based on RSSI vector similarity degree. Int J Distrib Sens Netw Aug 2014;10:371350.
- [61] Hoang MT, Yuen B, Dong X, Lu T, Westendorp R, Reddy K. Recurrent neural networks for accurate RSSI indoor localization. IEEE Internet Things J Dec 2019:6:10639–51.
- [62] Avila-Campos P, Astudillo-Salinas F, Vazquez-Rodas A, Araujo A. Evaluation of LoRaWAN transmission range for wireless sensor networks in riparian forests. In: Proceedings of the 22nd international ACM conference on modeling, analysis and simulation of wireless and mobile systems. ACM; Nov 2019.
- [63] Sundaram JPS, Du W, Zhao Z. A survey on LoRa networking: research problems, current solutions, and open issues. IEEE Commun Surv Tutor 2020;22(1):371–88.
- [64] Callebaut G, der Perre LV. Characterization of LoRa point-to-point path loss: measurement campaigns and modeling considering censored data. IEEE Internet Things J Mar 2020;7:1910–8.
- [65] Lavric A, Popa V. Performance evaluation of LoRaWAN communication scalability in large-scale wireless sensor networks. Wirel Commun Mob Comput Jun 2018;2018:1–9.

- [66] Lazaro M, Lazaro A, Villarino R. Feasibility of backscatter communication using Lo-RAWAN signals for deep implanted devices and wearable applications. Sensors Nov 2020;20:6342.
- [67] Slaný V, Lučanský A, Koudelka P, Mareček J, Krčálová E, Martínek R. An integrated IoT architecture for smart metering using next generation sensor for water management based on LoRaWAN technology: a pilot study. Sensors Aug 2020;20:4712.
- [68] Janssen T, BniLam N, Aernouts M, Berkvens R, Weyn M. LoRa 2.4 GHz communication link and range. Sensors Aug 2020;20:4366.
- [69] Gaelens J, Torre PV, Verhaevert J, Rogier H. LoRa mobile-to-base-station channel characterization in the Antarctic. Sensors Aug 2017;17:1903.
- [70] Masadan NAB, Habaebi MH, Yusoff SH. LoRa LPWAN propagation channel modelling in IIUM campus. In: 2018 7th international conference on computer and communication engineering (ICCCE). IEEE; Sep 2018.
- [71] Elijah O, Rahim SKA, Sittakul V, Al-Samman AM, Cheffena M, Din JB, et al. Effect of weather condition on LoRa IoT communication technology in a tropical region: Malaysia. IEEE Access 2021;9:72835–43.
- [72] Friis H. A note on a simple transmission formula. Proc IRE May 1946;34:254-6.
- [73] Harinda E, Hosseinzadeh S, Larijani H, Gibson RM. Comparative performance analysis of empirical propagation models for LoRaWAN 868mhz in an urban scenario. In: 2019 IEEE 5th world forum on Internet of things (WF-IoT). IEEE; Apr 2019.
- [74] Rappaport TS. Wireless communications-principles and practice, (the book end). Microw J 2002;45(12):128-9.
- [75] Goldsmith A. Wireless communications. Cambridge University Press; 2005.
- [76] Akin D, Bardwell J. Certified wireless network administrator: Official study guide. 2005.
- [77] Viswanathan M. Wireless communication systems in Matlab. Independently Published: 2018.
- [78] Semtech. LoRa and LoRaWAN: a technical overview. 2021.
- [79] Kim S, Lee H, Jeon S. An adaptive spreading factor selection scheme for a single channel LoRa modem. Sensors Feb 2020;20:1008.
- [80] Melling L. Peatland in Malaysia. In: Tropical peatland ecosystems. Japan: Springer; 2016. p. 59–73.
- [81] Page SE, Rieley JO, Banks CJ. Global and regional importance of the tropical peatland carbon pool. Glob Change Biol Jan 2011;17:798–818.
- [82] Phillips VD. Peatswamp ecology and sustainable development in Borneo. Biodivers Conserv 1998;7(5):651–71.
- [83] Adon R, Bakar I, Wijeyesekera DC, Zainorabidin A. Overview of the sustainable uses of peat soil in Malaysia with some relevant geotechnical assessments. International Journal of Integrated Engineering 2012;4(4).
- [84] Moayedi H, Nazir R. Malaysian experiences of peat stabilization, state of the art. Geotech Geolog Eng Jul 2017;36:1–11.
- [85] Shah ASN, Mustapha KA, Hashim R. Characterization and impact of peat fires on stabilization of tropical lowland peats in Banting, Selangor, Malaysia. Sains Malays Mar 2020;49:471–81.
- [86] Nuruddin AA, Musa DNS, Chua L. Recurrent burnt peat: potential positive feedback for peat fires. In: Proceedings of the 15th international peat congress: 2015.
- [87] Parish F, Lim SS, Perumal B, Giesen W. Summary RSPO manual on best management practices (bmps) for management and rehabilitation of natural vegetation associated with oil palm cultivation on peat. Roundtable on Sustainable Palm Oil (RSPO).
- [88] Yunus MA Md. Internet of things (IoT) application in meliponiculture. International Journal of Integrated Engineering Dec. 2017;9.
- [89] Kufakunesu R, Hancke GP, Abu-Mahfouz AM. A survey on adaptive data rate optimization in LoRaWAN: recent solutions and major challenges. Sensors Sep 2020;20:5044.



Nur Luqman Saleh is a Senior Lecturer in the Department of Computer and Communication System Engineering at the Faculty of Engineering, Universiti Putra Malaysia (UPM). He earned his Bachelor's degree in Electronic Engineering, specializing in Microwave and Communications, from Multimedia University (MMU), Cyberjaya, Malaysia, in 2012. In 2014, he obtained a Master's degree in Engineering Management from Universiti Putra Malaysia (UPM). He completed his Ph.D. in Communications and Network Engineering at UPM in 2020. His research interests include Radar and Microwave Communication Systems, Bio-

Inspired Signal Processing, Distributed Acoustic Sensing, and the Internet of Things. Prior to his academic career, he worked in the telecommunications industry.



Aduwati Sali is currently the Director of the Institute for Mathematics Research (INSPEM) at UPM. She is also a Professor in the Department of Computer and Communication Systems at UPM, where she has been since February 2019. Previously, she served as Deputy Director of UPM's Research Management Centre from 2016 to 2019. She holds a PhD in Mobile and Satellite Communications from the University of Surrey (2009), an MSc in Communications and Network Engineering from UPM (2002), and a BEng in Electrical and Electronics Engineering from the University of Edinburgh (1999). She is a Chartered Engineer reg-

istered with the UK Engineering Council and a Professional Engineer with the Board

of Engineers Malaysia. Her industry experience includes a role as Assistant Manager at Telekom Malaysia Bhd (1999-2000). Actively involved in IEEE, she has served as Chair of ComSoc/VTS Malaysia and Young Professionals. She is an Honorary Member of the Young Scientists Network-Academy of Sciences Malaysia and received the 2018 Top Research Scientists Malaysia Award. In 2020, she was a Visiting Scientist at the KIOS Research and Innovation Centre in Cyprus under the EU Horizon2020-RISE project.



Jiun Terng Liew is currently a freelance app developer. Previously, he worked as a Research Associate in the Department of Computer and Communication System Engineering at the Faculty of Engineering, Universiti Putra Malaysia. He earned his PhD in Computer Networks from UPM in April 2020. During his PhD studies, he spent a total of one year as a research associate at the University of York, participating in the EU Horizon 2020-RISE project. He received his B.S. in Computer and Communication System Engineering with first-class honors from UPM in 2014. His research interests include machine-to-machine networks, media

access control protocols, radio resource allocation in wireless networks, and performance analysis.



Sharifah Mumtazah Syed Ahmad received her Ph.D. in Electronics from University of Kent, United Kingdom. She is currently an Associate Professor, in Department of Computer and Communication Systems Engineering, Faculty of Engineering in Universiti Putra Malaysia. She is the member of the NAPC: Network ASEAN Peat Swamp Forest Communities projects from 2018 until now. Her research interests include machine learning and data analytics. She has published numerous journals and research proceedings as well as a patent in Biometrics Security.



Azizi Mohd Ali is currently the Head of Funding at the Research Management Center (RMC) at Universiti Putra Malaysia (UPM). He also works as a Research Officer at the Wireless and Photonics Networks Research Centre (WiPNET) at UPM. Azizi holds a Bachelor of Engineering in Computer and Communication Systems from UPM. Previously, he was a Senior Engineer in Radio Planning and Network Optimization at Nokia Siemens Networks, focusing on 2G, 3G, TETRA, and WiMAX networks. His research interests include Wireless Sensor Networks, IoT, and Wireless Communication.



Borhanuddin Mohd Ali earned his BSc (Hons) in Electrical and Electronics Engineering from Loughborough University of Technology in 1979, followed by an MSc and PhD from the University of Wales, Cardiff, in 1982 and 1985, respectively. He is currently serving as a professor on a post-retirement contract in the same department. A Senior Member of IEEE and a member of the IET, he is also a Chartered Engineer and a Fellow of the Academy of Sciences Malaysia. His research interests include Wireless Sensor Networks (WSN), IoT, Wireless Resource Management, Mobility Management, Cognitive Radio, and Massive

MIMO and 5G. He has published over 300 papers in refereed journals and conferences.



Ahmad Ainuddin Nuruddin earned his B.S. in Microbiology in 1982 and M.S. in Environment in 1985 from Ohio University. He completed his Doctorate in Forestry, specializing in Microclimatology, at Stephen F. Austin State University in 1996. With over 130 peer-reviewed articles and book chapters to his name, he has actively contributed to various national and international conferences. His research expertise encompasses microclimatology and forest fire management, through which he has secured RM 1.9 million in funding from diverse research agencies. His ac-

colades include the Canadian Forest Service Merit Award from

the Minister of Environment Canada for his adaptation of the Canadian Forest Fire Index to Malaysia's context. Additionally, he has received the Universiti Putra Malaysia Excellence Service Award in 1997, 2003, 2008, 2013, and 2016, along with travel grants from prestigious organizations such as UNESCO-MAB, JSPS, KFRI, EU-COST, IUFRO, ITTO, and the Korean Government.



Sheriza Mohd Razali holds a B.Sc. in Forest Management and an M.Sc. in the Application of Remote Sensing and GIS from Universiti Putra Malaysia. She completed her Ph.D. in Biodiversity and Environmental Management (Remote Sensing and GIS) at Universidad de Murcia, Spain. Currently, she serves as a Research Officer at the Institute of Tropical Forestry and Forest Products, Universiti Putra Malaysia. Previously, she worked as a Research Officer at the Malaysian Remote Sensing Agency from 2002 to 2003. Since 2018, she has been a member of the Fundamental Research Grant Scheme (FGRS), Transdisciplinary Research

Grant Scheme (TGRS), and the NAPC: Network ASEAN Peat Swamp Forest Communities projects. She is also the project leader for a hydrological modeling study for Ulu Muda Forest Reserve, a collaboration involving WWF Malaysia, UPM, and Universiti Malaysia Terengganu. Her research focuses on remote sensing and GIS, and she is proficient in ArcGIS, ERDAS, and ENVI software. Sheriza has published 18 journal articles, a book, five book chapters, 18 conference proceedings, and seven other publications.



Nordin Ramli is an award recipient of the Top Research Scientist Malaysia (TRSM) and Young Scientist Network (YSN) honors from the Academy of Sciences Malaysia in 2018 and 2014, respectively. He earned his B.Eng. in Electrical Engineering from Keio University, Japan, in 1999, followed by M.Eng. and Ph.D. degrees in Electronic Engineering in 2005 and 2008. With over 20 years of experience in the telecommunications industry, Nordin has worked as a network engineer at Telekom Malaysia Berhad (1999-2008) and as a lecturer at Multimedia University (2008-2009). He currently serves as a Senior Staff Researcher at the

Wireless Innovation Department of MIMOS Berhad, managing R&D for in-house technology development focused on IoT and big data projects. His research interests include cognitive radio, TV white space, adaptive systems, wireless mesh networking, and 5G. Nordin has published around 100 papers and filed over 30 patents related to wireless communications. He is also an Associate Editor for the IEICE Communication Express (COMEX) and a Senior Member of IEEE.